Supporting Information

Engineering interface-mediated heterojunction in MOF-derived C-In_2O_3 microrods and CdS nanoclusters for enhanced photocatalytic H_2O_2 production

Qipiao Zhang[a #], Tao Lei[a #], Hongli Yang[a], Zihao Yuan[a], Jiahao Song[a], Enze Hu[a], Hongfei Bao[a], Dongdong Zhang[a], Huilin Hou[a], Weiyou Yang[a], Zhao Liang[a*], Xiaoqiang Zhan[a*]*

[a]*Institute of Micro/Nano Materials and Devices, Ningbo University of Technology, Ningbo, 315211, P. R. China*

[*]Corresponding authors. E-mails: cumtmaterial@163.com (H. Yang) walleliang@hnu.edu.cn (Z. liang) and zhanxiaoqiang777@163.com (X. Zhan)

[#] These authors contribute equally

Tel: +86-574-87080966, Fax: +86-574-87081221.

Experimental Procedure

Materials

Indium (III) nitrate hydrate ($In(NO_3)_3 \cdot xH_2O$, A.R., Aladdin), N, N-dimethylformamide (DMF, A.R., Aladdin), terephthalic acid (H_2BDC, A.R., Aladdin), Cadmium acetate ($(CH_3COO)_2Cd$, A.R., Aladdin), Sodium sulfide ($Na_2S \cdot 9H_2O$, A.R., Aladdin), Ethanol anhydrous (CH_3CH_2OH, 99.7%, Macklin), potash iodide (KI, A.R., Aladdin), Potassium acid phthalate ($C_8H_5O_4K$, AR, Macklin), Hydrogen peroxide (30%, AR, XILONG SCIENTIFIC), deionized water (Millipore, 18.2 MΩ cm). The above chemicals were used directly and no further purification was carried out.

Characterization

Field emission scanning electron microscopy (FESEM) (Hitachi, Japan) transmission electron microscopy (TEM), and high-resolution transmission electron microscopy (HRTEM) using the JEOL JEM-F200 (Japan) were hired to observe the microstructure and morphology of the samples. X-ray power diffraction (XRD) patterns were obtained using the Bruker D8 Advance instrument from Germany with Cu Ka radiation (l = 1.5406 Å) to determine the crystal structures. X-ray photoelectron spectroscopy (XPS) was conducted using the Thermo Fisher Scientific ESCALAB 250Xi instrument from America to analyze the surface species and chemical states. Diffuse reflectance absorption spectra were measured on a Hitachi UV-3900 UV-visible spectrophotometer with an integrated sphere attachment, employing BaSO4 as the reflectance standard. The specific surface area of the materials was calculated using the adsorption data in the pressure range of P/P_0 = 0 - 1 by the Brunauer-Emmett-Teller (BET) model. Pore size distribution was obtained by the Barrett-Joyer-Halenda (BJH) model using the adsorption branch of the isotherm. The room temperature electron paramagnetic resonance (EPR) spectra of the samples were measured by Bruker EMXplus-6/1. Photoluminescence (PL) spectra were measured on Edinburgh FLS1000 fluorescence spectrometer with an excitation wavelength of 350 nm. Time-resolved photoluminescence (TRPL) spectra were collected on Edinburgh FLS1000 fluorescence spectrometer with an excitation wavelength of 470 nm.

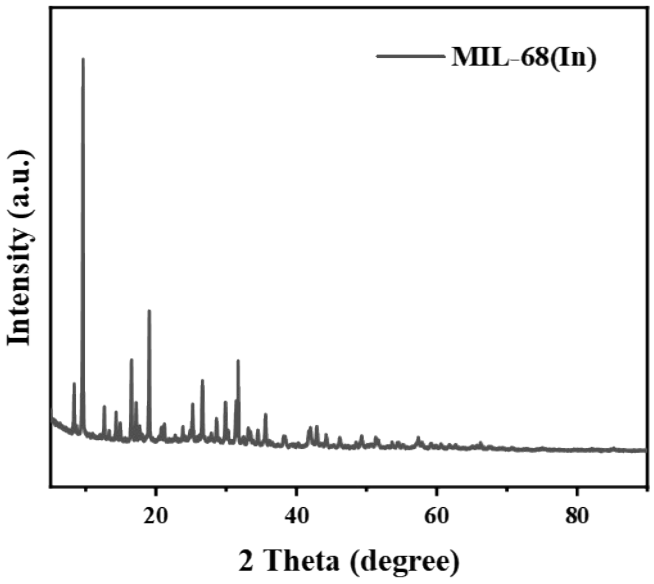

Fig. S1 XRD spectra of as-prepared MIL-68(In).

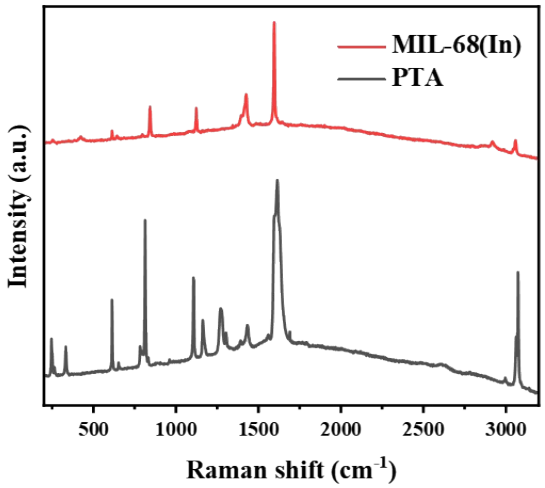

Fig. S2 Raman spectra of as-prepared MIL-68(In) and PTA.

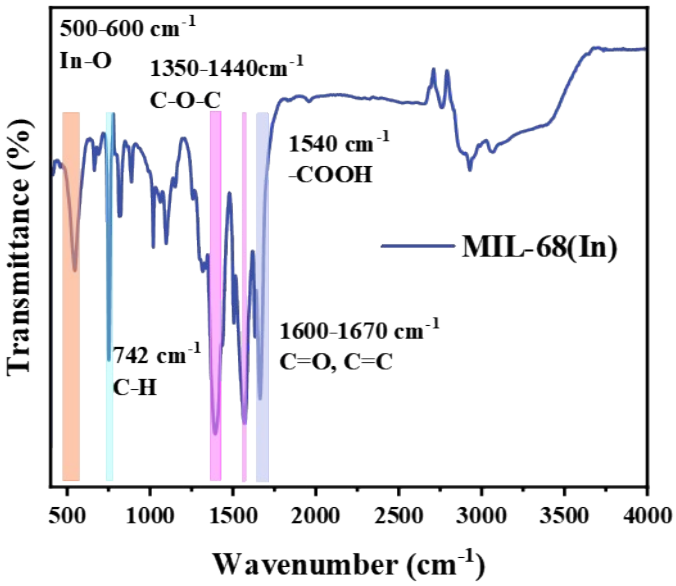

Fig. S3 FT-IR spectra of as-prepared MIL-68(In).

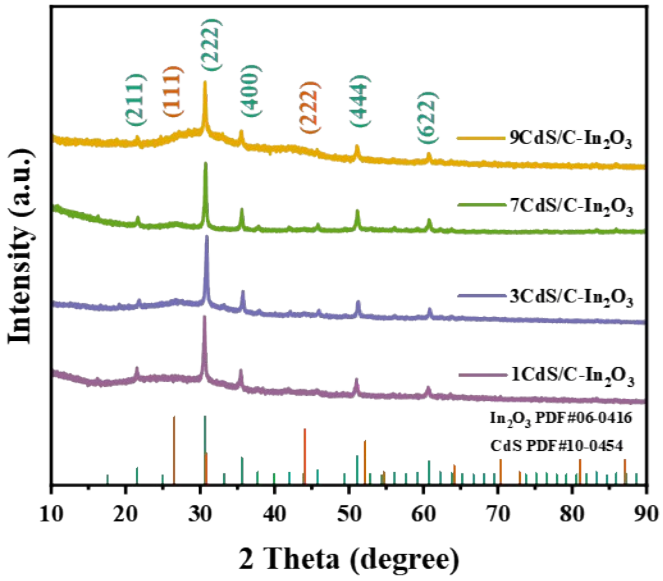

Fig. S4 XRD patterns of as-prepared CdS/C-In_2O_3

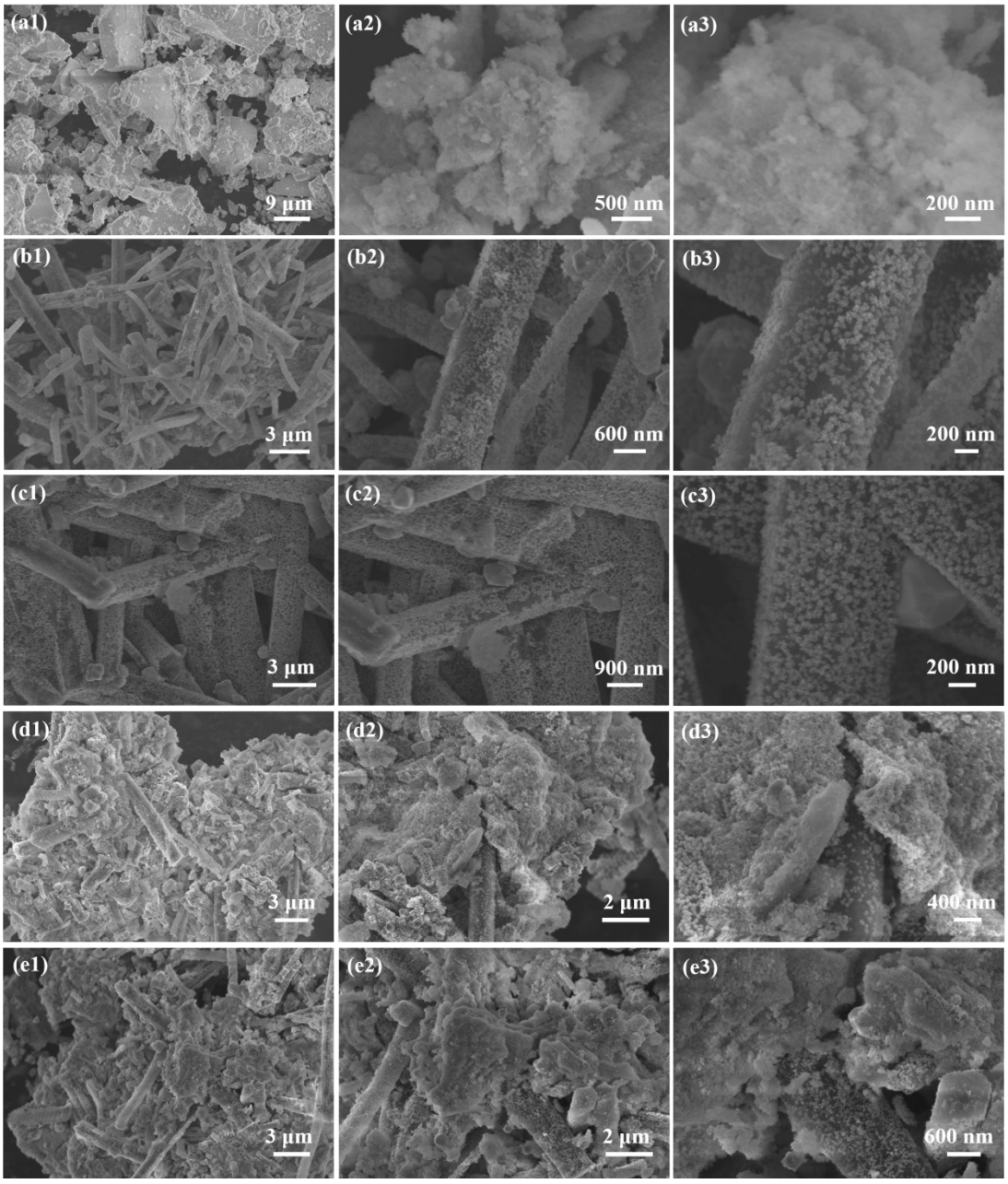

Fig. S5 Typical SEM images of (a) CdS, (b) 1CdS/C-In_2O_3, (c) 3CdS/C-In_2O_3, (d) 7CdS/C-In_2O_3, (e) 9CdS/C-In_2O_3.

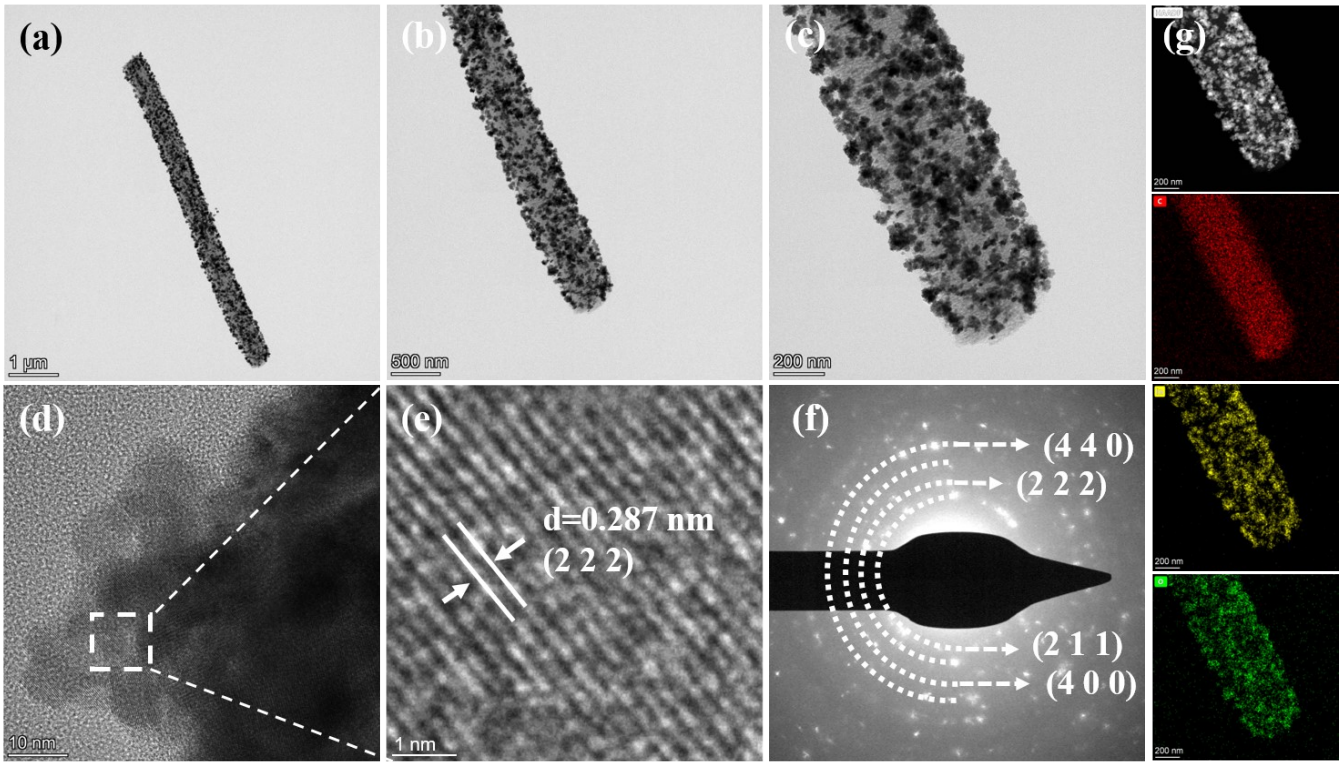

Fig. S6 (a-d) Typical TEM images of C-In_2O_3. (e) Typical HRTEM images recorded from the marked area in (d). Corresponding (f) SAED spectrum of C-In_2O_3. (g) Elemental mappings corresponding to the selected area of C-In_2O_3.

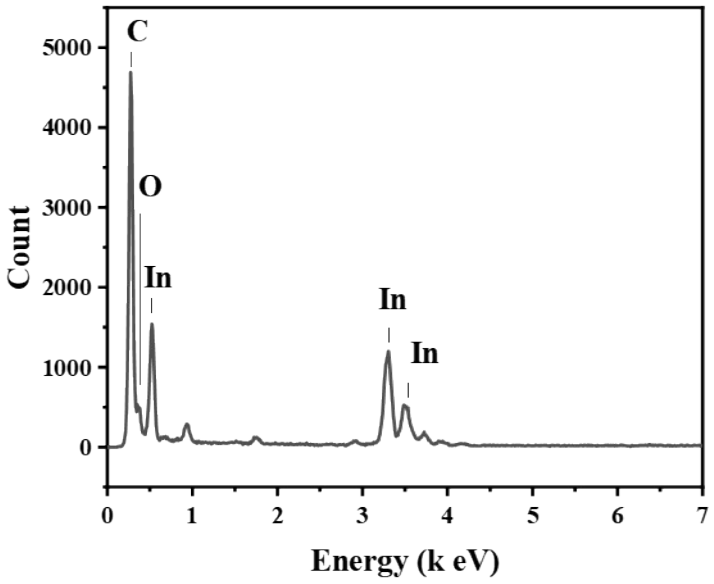

Fig. S7 EDX spectrum of C-In_2O_3.

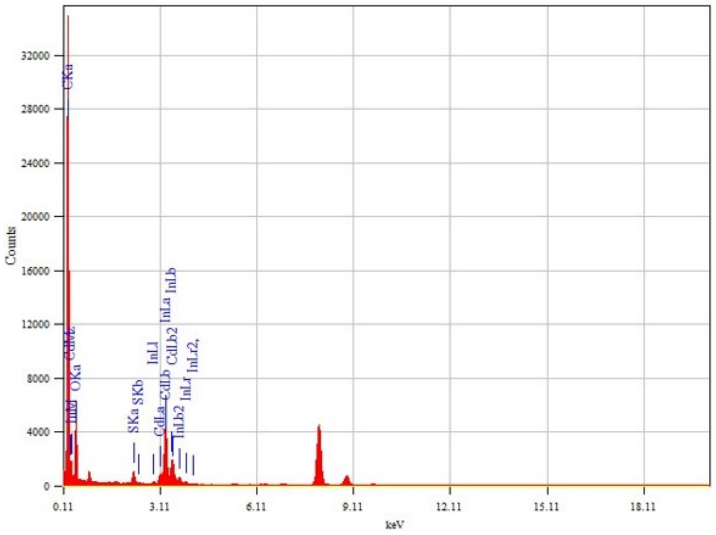

Fig. S8 EDX spectrum of 5CdS/C-In_2O_3.

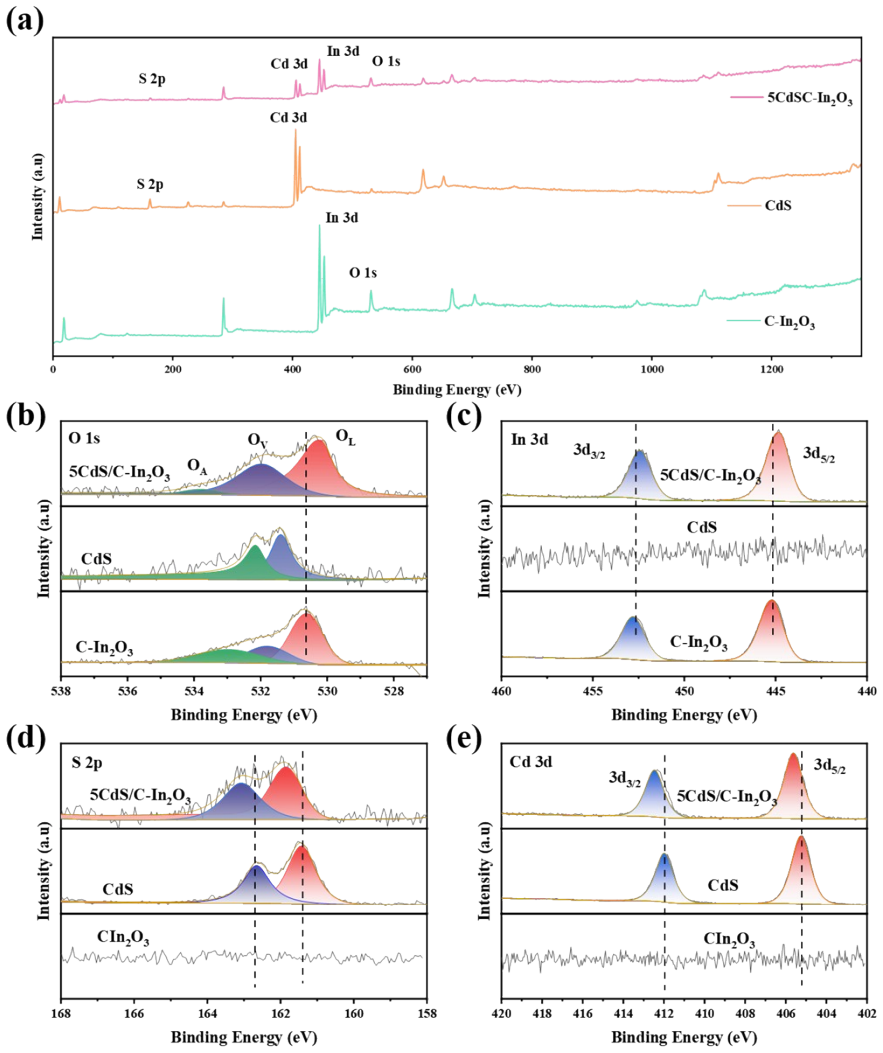

Fig. S9 (a-d) XPS spectra of as-prepared C-In_2O_3, CdS and 5CdS/C-In_2O_3. (a-d) High-resolution XPS spectra of In 3d (a), O 1s (b), Cd 3d (c), S 2p (d) of as-prepared C-In_2O_3, CdS and 5 CdS/C-In_2O_3, respectively.

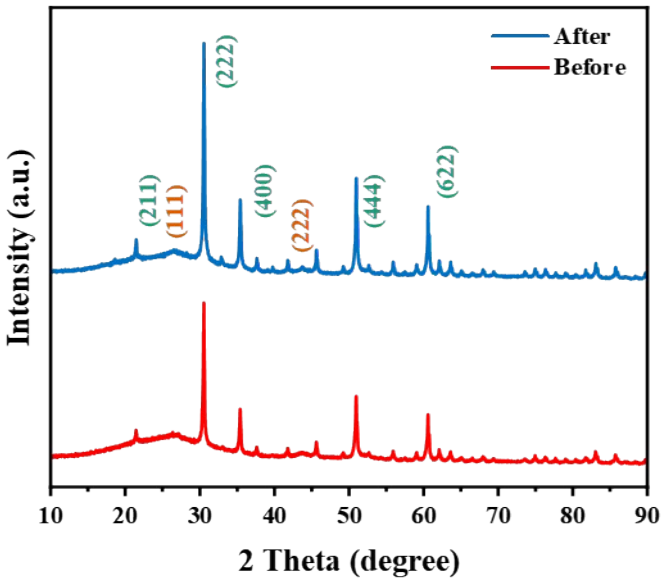

Fig. S10 XRD spectra of 5CdS/C-In_2O_3 after test.

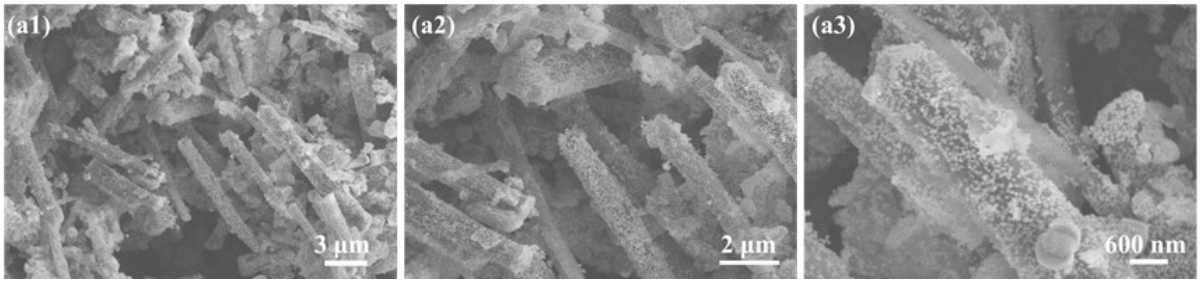

Fig. S11 SEM image of 5CdS/C-In_2O_3 after test.

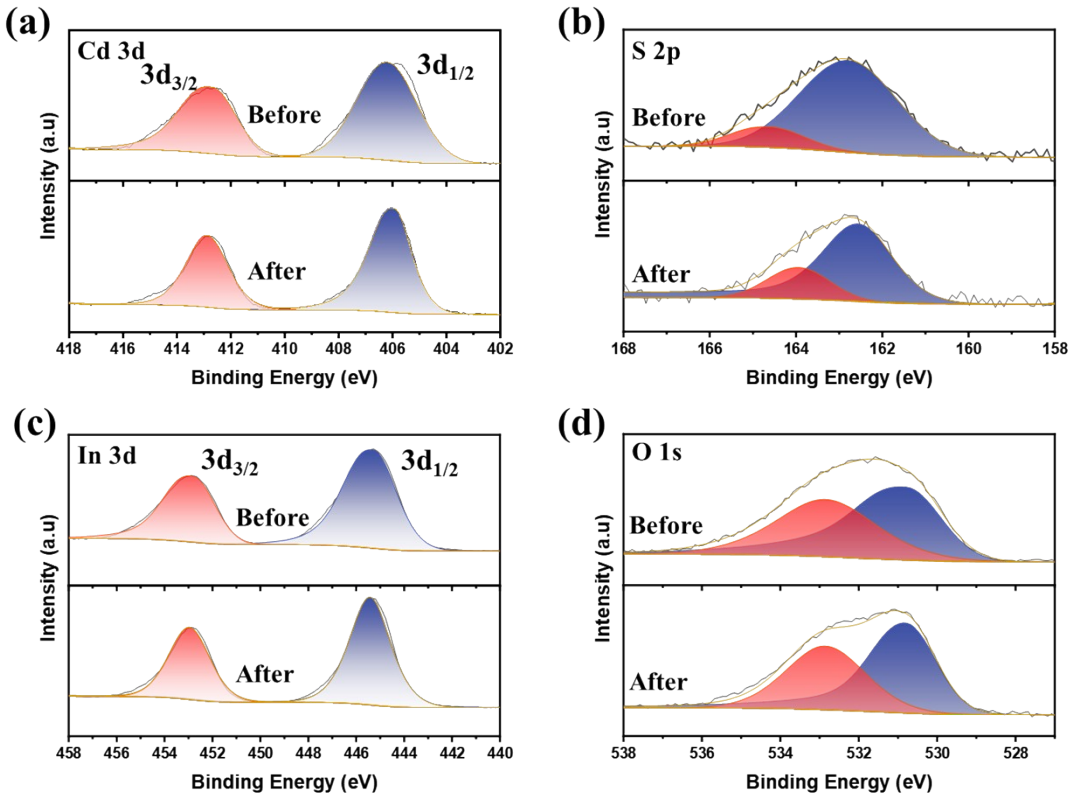

Fig. S12 Comparison of XPS spectra of 5CdS/C-In_2O_3 before and after the reaction. (a-d) High-resolution XPS spectra of Cd 3d (a), S 2p (b), In 3d (c), O 1s (d) of 5 CdS/C-In_2O_3, respectively.

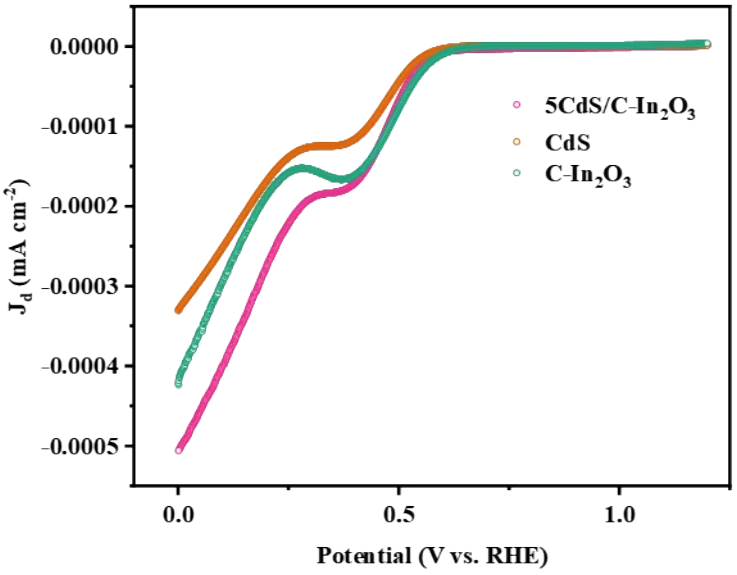

Fig. S13 RRDE polarization curves over C-In_2O_3, CdS and 5CdS/C-In_2O_3 in O_2-saturated 0.1 M KOH (pH = 12.9) at 1600 rpm with ring current (upper part) and density of disk current.

Table S1 experimental details for experimental details for AQY test

wave length (nm)	H_2O_2 yield (mol)	Time（s）	optical power density (W/cm^2)	Area (cm^2)	velocity of light C	Planck constant h	Number of incident photons	H_2O_2 molecules	AQY (%)
400	2.69764E-05	3600	0.0126	7.065	300000000	6.626E-34	6.44871E+20	3.24795E+19	5.0365994 55
450	2.19446E-05	3600	0.0126	7.065	300000000	6.626E-34	7.25479E+20	2.64213E+19	3.6419091 8
500	5.54028E-06	3600	0.0118	7.065	300000000	6.626E-34	7.54908E+20	6.6705E+18	0.8836172 24
550	2.39543E-06	7200	0.0138	7.065	300000000	6.626E-34	1.94229E+21	2.88409E+18	0.1484893 94

Table S2 Comparison of photocatalytic H_2O_2 production rate of CdS/C-In_2O_3 heterostructure with recent reported photocatalysts.

Catalyst	H_2 Evolution ($\mu mol \cdot g^{-1} \cdot h^{-1}$)	Sacrificial agent	Photosensitizer Cocatalyst	Light Source	Ref.
In_2S_3@In_2O_3	275	\	\	$\lambda \geq 420$ nm	[1]
In_2O_3/$ZnIn_2S_4$	590	\	\	$\lambda \geq 420$ nm	[2]
In_2O_3/$ZnIn_2S_4$	5716	1 mM Na_2SO_3 and Na_2S	\	$\lambda \geq 420$ nm	[3]
Ag-$ZnIn_2S_4$/C-In_2O_3	2420	10 vol% isopropanol	\	$\lambda \geq 420$ nm	[4]
This work	2343	isopropanol	\	$\lambda \geq 420$ nm	

Table S3 τ_1 and τ_2 were fitted with the a biexponential decay model delivered form software and the average lifetime (τ_a) was obtained using the equation: $\tau_a = \frac{A_1\tau_1^2 + A_2\tau_2^2}{A_1\tau_1 + A_2\tau_2}$.

photocatalyst	τ_1	τ_2	τ_a
C-In_2O_3	1.07	16.45	3.31
CdS	1.60	22.30	4.64
5CdS/C-In_2O_3	1.21	8.57	2.38

References

1. X. Chen, W. Zhang, L. Zhang, L. Feng, C. Zhang, J. Jiang and H. Wang, ACS Appl. Mater. Interfaces, 2021, 13, 25868-25878.
2. S. Liu, Y. Mao, Q. Han and X. Liu, Materials Science in Semiconductor Processing, 2024, 170, 107978.
3. R. Bariki, K. Das, S. K. Pradhan, B. Prusti and B. G. Mishra, ACS Appl. Energy Mater., 2022, 5, 11002-11017.
4. T. Lei, X. Zhan, Z. Yuan, Z. Wang, H. Yang, D. Zhang, Y. Li, W. Yang, G. Lin and H. Hou, Sep. Purif. Technol., 2025, 359, 130474.